Hindawi
Mathematical Problems in Engineering
Volume 2020, Article ID 9839341, 11 pages
https://doi.org/10.1155/2020/9839341

Research Article

Modeling of Tension Control System with Passive Dancer Roll for Automated Fiber Placement

Yi Liu, Qiang Fang, and Yinglin Ke

The State Key Lab of Fluid Power Transmission and Control, School of Mechanical Engineering, Zhejiang University, Hangzhou, China

Correspondence should be addressed to Qiang Fang; fangqiang@zju.edu.cn

Received 3 December 2019; Revised 7 March 2020; Accepted 25 March 2020; Published 30 April 2020

Academic Editor: Salvatore Strano

The fiber tension should be kept constant during the automated placement of fiber prepreg. The velocity of the fiber placement end-effector moving on complex aircraft panel mould surface varies rapidly, which greatly disturbs the precision of tension control. This paper proposes a tension control strategy combining active control and passive control. The pay-off motor controls the fiber tension directly and a passive dancer roll is designed theoretically as the equipment for attenuation of tension disturbance to realize the real-time compensation of low-frequency velocity variations. The nonlinear model of tension control system, which includes the dynamics of the passive dancer roll, is established, and the effect of dancer roll parameters on its disturbances attenuation performance is analyzed. The controller is designed using the H_∞ mixed sensitivity method. An experimental tension control precision about 2% is obtained at stable placement speed on the automated fiber placement (AFP) machine. The experiments also indicated that the tension would not vary over 1 N at a maximum acceleration of 4 m/s^2.

1. Introduction

Composite materials are widely used for aeronautic application, and the automated fiber placement (AFP) is especially suitable for the manufacture of large composite structures, such as fuselage and S-shaped inlet, due to its high efficiency, high quality, and strong adaptability [1, 2]. The fiber tension has important influence on the strength and fatigue resistance of composite materials, because the tension variations may lead to wrinkles and other defects, even cause the fiber to break [3, 4]. The damage to the fiber increases as the tension increases in the placement process, and higher tension on the fiber results higher breakage and neps [5]. However, tension and velocity of the fiber are strongly coupled, and the drastic change of placement velocity will affect the tension stability, so it is of great significance to control the fiber tension accurately during the highly efficient placement.

The research on tension control has many achievements in the fields of textile, printing, wire-cutting, and fiber winding. Chen et al. [6] presented a hybrid adaptive iterative learning control scheme for a double-rope winding hoisting system driven by permanent magnet synchronous motor systems and established the mathematical model of the system based on the discrete model of the wire rope. Pagilla et al. [7] presented an accurate dynamics model for the unwind roll and a decentralized control strategy based on the reference tension of each zone. Tran and Choi [8–10] proposed an improved mathematical model for roll-to-roll system in printing industry and designed tension controller using backstepping method to realize precise tension control of paper. Yan [11] presented a one-step-ahead adaptive controller to guarantee smooth wire transport and a constant tension value for wire electrical discharge machining. In general, in a multispan roll-to-roll system, a plurality of actuators and senor signals are provided in the tension control to handle tension disturbances between different spans, in particular the moment or speed of the end roller being controlled and measured. This is beneficial to improve the precision and robustness of tension control.

Dancer rolls are widely used in fiber feeding systems, including active dancers and passive dancers, distinguished

by the external actuator. The dancer roll can attenuate the disturbances, but also be used as a tension measuring module to replace the tension sensor. Shin [12] studied the mathematical model of a passive dancer roll system and explored the frequency range when the dancer roll is used for tension measurement. Ebler et al. [13] compared the two schemes using tension sensor and dancer roll as tension measurement module. The experimental results show that the former combined with a suitable filter can obtain better control effect. Shelton [14] analyzed the limitations of the passive dancer roll as a sensor for the tension measurement. Kang et al. [15] established the model of hybrid roll system model composed of passive dancer roll and active dancer roll, and verified its performance with PI controller. Dwivedula et al. [16] compared the difference between passive dancers roll and active dancer roll in disturbances attenuation and found that the active dancer roll is more effective in attenuation of high-frequency disturbance. However, the disturbance is treated as tension disturbance directly, which leads to inaccurate guidance results. Gassmann et al. [17] studied a tension control system with swing active dancer roll. The position controller of dancer roll-based position feedback is designed by means of mixed sensitivity method. Thiffault et al. [18] adopted an active dancer roll to reduce the sensitivity to voltage sags in winding systems. In addition to mechanism improvement, some typical advanced control techniques are also used in tension control, such as linear parameter varying (LPV) control [19], H_∞ control [17], parameter adaptive estimation [20], artificial neural nets [21], nonlinear dynamic matrix control [22], fuzzy logic control [23], and adaptive sliding mode control [24]. These control methods have been proved to improve the robustness and accuracy of tension control system.

Generally speaking, the traditional roll-to-roll system is usually a multi-input multioutput system. The torque or speed of unwinding roll and rewinding roll are controllable and measurable. There are also multiple actuators between spans to reduce disturbances, and the precision and robustness of tension control can be effectively ensured by controlling the speed difference of rolls and adjusting the position of the active dancer roll. Different from roll-to-roll systems, the end-effector of AFP (shown in Figure 1) has 16 sets of fiber feeding mechanisms, distributed evenly and symmetrically along the center axis, and the 16 lanes of fiber are transported to the end compaction roll for placement. The motion path of the end-effector is planned according to the surface of the aircraft panel mould, and the rewinding speed depends on the compaction roll with the AFP moving, so the precise control and measurement of the speed of placement is not feasible. In addition, 16 lanes of fiber are placement side by side, and there are differences in the velocity of different fiber, considering the eccentricity and nonroundness of the compaction roll. The tension closed-loop control strategy based on tension signal feedback for AFP is adopted in this paper, which only depends on the pay-off motor to control the fiber tension. Different from the speed difference control or the dancer roll position control, the stability of direct tension control is easily affected by

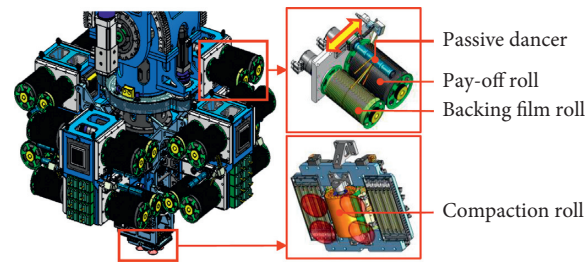

Figure 1: 16-Lane fiber placement end-effector.

velocity changing during placement process, because the bandwidth of the servo motor is limited. In order to reduce the sensitivity of tension system to the change of downstream placement velocity, the passive dancer roll without driving mechanism is equipped to attenuate the velocity disturbance on the premise that the end-effector remains light and compact. These passive dancer rolls can make up for the weakness of limited bandwidth of pay-off motor and the attenuation ability of the disturbance is related to the mechanical parameters of the dancer roll. Although there are studies on the function and performance of linear or swing dancer roll, little attention has been paid to the attention of passive dancer roll to the disturbance caused by the downstream velocity variation in a tension closed-loop control system. It is necessary to achieve the design guidance of passive dancer roll used in the end-effector of AFP.

Thus, the tension control system with passive dancer roll for the AFP is designed in this paper, and the attention mechanism of passive dancer roll to downstream velocity disturbance is discussed. The tension physical model including dynamic model of dancer roll is established firstly, and the attention performance of dancer roll is analyzed based on this model. The design of the fiber feeding mechanism is improved using the guidance for mechanical design of passive dancer roll. Considering the modeling uncertainty and external disturbance caused by guide rolls, the force controller of the pay-off motor is designed using the standard H_∞ method. The robustness and tracking precision of tension control system equipped passive dancer roll are proved by experiments on the AFP.

2. System Modeling

The fiber feeding system of the AFP includes the pay-off roll, the passive dancer roll, the tension sensor, guide rolls, and the compaction roll, as shown in Figure 2. The pay-off roll is driven by a servo motor, and the tension sensor is used for tension measurement. The tension stability control in the placement process is realized by adjusting the output torque of the pay-off motor.

The model for the tension control system is based on three laws:

(i) Hooke's law, which models the elasticity of the fiber

(ii) Mass conservation law, which expresses that the mass of the fiber remains constant between the state without stress and the state under stress

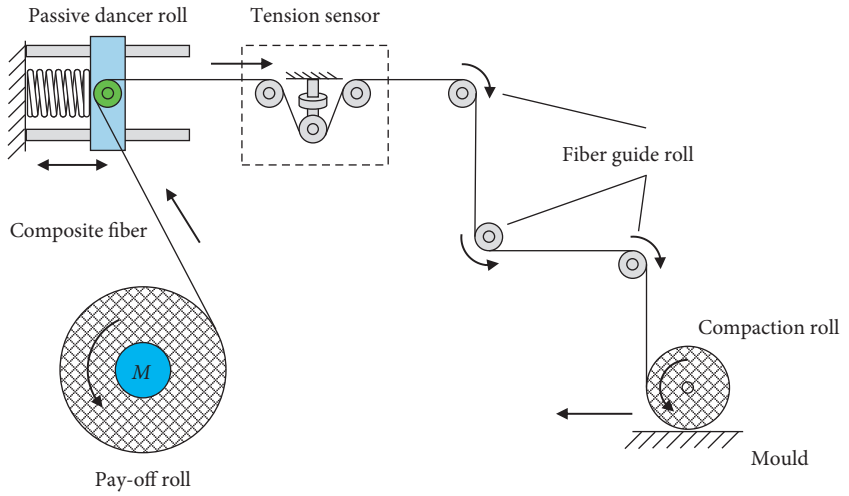

Figure 2: Tension control sketch for modeling.

(iii) Newton's law, which gives the passive dancer's position and velocity variation due to the fiber tension

2.1. Tension Model of the Fiber. According to the mass conservation law, the mass of fiber between two rolls is conserved, which can be expressed as

$$\frac{\mathrm{d}}{\mathrm{d}t}\frac{L_k\rho_k A_k}{1+\varepsilon_k} = \frac{\rho_k A_k v_{k-1}}{1+\varepsilon_{k-1}} - \frac{\rho_k A_k v_k}{1+\varepsilon_k}, \tag{1}$$

where k is the roll number, v_k is the velocity of fiber on the k^{th} roll, L_k, ρ_k, A_k, and ε_k are, respectively, the span length, density, cross-sectional area, and strain of fiber between the $(k-1)^{\text{th}}$ roll and the k^{th} roll. The relationship can be simplified as

$$\frac{\mathrm{d}}{\mathrm{d}t}\frac{L_k}{1+\varepsilon_k} = \frac{v_{k-1}}{1+\varepsilon_{k-1}} - \frac{v_k}{1+\varepsilon_k}. \tag{2}$$

This relationship can be simplified by differentiating the left term

$$\frac{1}{1+\varepsilon_k}\frac{\mathrm{d}L_k}{\mathrm{d}t} - \frac{L_k}{(1+\varepsilon_k)^2}\frac{\mathrm{d}\varepsilon_k}{\mathrm{d}t} = \frac{v_{k-1}}{1+\varepsilon_{k-1}} - \frac{v_k}{1+\varepsilon_k}. \tag{3}$$

So the final relationship can be expressed as

$$L_k\frac{\mathrm{d}\varepsilon_k}{\mathrm{d}t} = (1+\varepsilon_k)v_k - \frac{(1+\varepsilon_k)^2}{1+\varepsilon_{k-1}}v_{k-1} + (1+\varepsilon_k)\frac{\mathrm{d}L_k}{\mathrm{d}t}. \tag{4}$$

Using the approximations $\varepsilon_0, \varepsilon_1, \varepsilon_2 \ll 1$, $(1+\varepsilon_k)^2/1+\varepsilon_{k-1}) \approx (1-\varepsilon_{k-1})(1+2\varepsilon_k)$ [19], and equation (4), we can obtain

$$L_k\frac{\mathrm{d}\varepsilon_k}{\mathrm{d}t} = (1+\varepsilon_k)\left(v_k - v_{k-1} + \frac{\mathrm{d}L_k}{\mathrm{d}t}\right) + v_{k-1}(\varepsilon_{k-1} - \varepsilon_k). \tag{5}$$

We can see that L_k is constant without the passive dancer roll, and there is no "$\mathrm{d}L_k/\mathrm{d}t$." As a result of the movement of the dancer roll, the downstream the upstream and downstream spans length has changed, as shown in Figure 3. The solid line represents the initial position of the dancer roll and the dashed line represents the position after it has moved x to the right. According to the trigonometric function of geometric relation, the upstream span changes can be obtained as

$$L_1' = L_1 - \delta L_1 = \frac{\sin\theta \cdot L_1 - x}{\sin(\theta - \delta\theta)}. \tag{6}$$

In general, the translation distance of the dancer roll is far less than the length of the spans, so $\delta\theta$ can be assumed to be very small, and thus $\cos\delta\theta \approx 1$ and $\sin\delta\theta \approx 0$ can be obtained. Based on this assumption, equation (2) can be expressed as

$$L_1' = L_1 - \delta L_1 = L_1 - \frac{x}{\sin\theta}. \tag{7}$$

Similarly, the downstream variation caused by the dancer roll's displacement can be expressed as

$$L_2' = L_2 - \delta L_2 = L_2 - x. \tag{8}$$

Therefore, the variation in length due to the movement of the dancer roll is given by

$$\frac{\mathrm{d}L_1}{\mathrm{d}t} = -\frac{1}{\sin\theta}\frac{\mathrm{d}x}{\mathrm{d}t}, \tag{9}$$

$$\frac{\mathrm{d}L_2}{\mathrm{d}t} = -\frac{\mathrm{d}x}{\mathrm{d}t}. \tag{10}$$

Substituting equations (9) and (10) into equation (5) results in

$$\begin{aligned} L_1\frac{\mathrm{d}\varepsilon_1}{\mathrm{d}t} &= (1+\varepsilon_1)\left(v_1 - v_0 - \frac{\dot{x}}{\sin\theta}\right) + v_0(\varepsilon_0 - \varepsilon_1), \\ L_2\frac{\mathrm{d}\varepsilon_2}{\mathrm{d}t} &= (1+\varepsilon_2)(v_2 - v_1 - \dot{x}) + v_1(\varepsilon_1 - \varepsilon_2). \end{aligned} \tag{11}$$

Under the assumption that the fiber is elastic, i.e., $\varepsilon_k = t_k/EA$, where E is the Young's modulus, the tension in

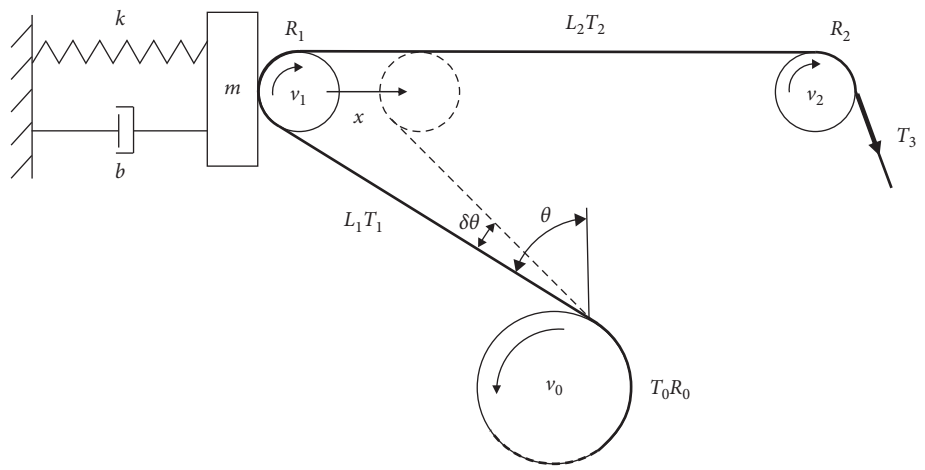

Figure 3: Passive dancer system.

the fiber on the upstream and downstream of the dancer roll can be expressed as

$$\frac{dt_1}{dt} = \frac{1}{L_1}\left[(EA + t_1)\left(v_1 - v_0 - \frac{\dot{x}}{\sin\theta}\right) + v_0(t_0 - t_1)\right], \quad (12)$$

$$\frac{dt_2}{dt} = \frac{1}{L_2}\left[(EA + t_2)(v_2 - v_1 - \dot{x}) + v_1(t_1 - t_2)\right]. \quad (13)$$

Equations (12) and (13) are nonlinear involving cross-product terms such as $v_i t_i$. To obtain linearized equations around nominal reference values of fiber velocity (V_{i0}) and fiber tension (T_{i0}), let $V_i = v_i - V_{i0}$, $T_i = t_i - T_{i0}$ for $i = 0, 1, 2$, where V_i and T_i represent the deviations [15, 19] (in fact, the nominal reference values in all the fiber spans are defined as equal: $V_{00} = V_{10} = V_{20}$, $T_{00} = T_{10} = T_{20}$).

Substituting V_i and T_i into equations (12) and (13), we obtain the linearized dynamics of fiber spans upstream and downstream to the dancer roller as

$$\begin{aligned} L_1\frac{dT_1}{dt} &= (EA + T_{10})\left(V_1 - V_0 - \frac{\dot{x}}{\sin\theta}\right) + V_{10}(T_0 - T_1) + \left[T_1\left(V_1 - V_0 - \frac{\dot{x}}{\sin\theta}\right) + V_0(T_0 - T_1)\right], \\ L_2\frac{dT_2}{dt} &= (EA + T_{20})(V_2 - V_1 - \dot{x}) + V_{20}(T_1 - T_2) + \left[T_2(V_2 - V_1 - \dot{x}) + V_1(T_1 - T_2)\right]. \end{aligned} \quad (14)$$

Since the system state near the equilibrium point is selected in the linearization process, deviations V_i and T_i are very small, and approximation equations can be got by omitting higher order terms and the remainder

$$\frac{dT_1}{dt} = \frac{1}{L_1}\left[(EA + T_{10})\left(V_1 - V_0 - \frac{\dot{x}}{\sin\theta}\right) + V_{10}(T_0 - T_1)\right], \quad (15)$$

$$\frac{dT_2}{dt} = \frac{1}{L_2}\left[(EA + T_{20})(V_2 - V_1 - \dot{x}) + V_{20}(T_1 - T_2)\right]. \quad (16)$$

2.2. Velocity Model of the Fiber. Assuming that the fiber does not slip on the roll, the velocity model of the fiber on the k^{th} roll can be expressed as follows according to the moment balance relationship:

$$J_k\frac{d}{dt}\left(\frac{v_k}{R_k}\right) = R_k(T_{k+1} - T_k) - B_f\frac{v_k}{R_k}, \quad (17)$$

where J_k, R_k, and B_f are, respectively, the inertia, radius, and bearing friction coefficient of the k^{th} roll.

2.3. Velocity Model of the Passive Dancer Roll. The dancer roll is subjected to the fiber tension, the spring force, and the guide force of the linear guide, so the force balance equation in the horizontal direction can be expressed as

$$m\ddot{x} = (\sin\theta\, T_1 + T_2) - b\dot{x} - kx. \quad (18)$$

The complete model of fiber feeding system can be built using the equations above. The tension T_0 is provided by the pay-off motor as the control input of system, and the tension T_2 in the downstream of dancer roll is measured by the tension sensor as the output of system. Taking the Laplace transform of equations (15)–(18) and the transfer functions of T_1 and T_2 can be expressed as

$$T_1(s) = H_1(s)T_0(s) + H_2(s)T_2(s), \quad (19)$$

$$T_2(s) = H_3(s)T_1(s) + H_4(s)V_2(s), \quad (20)$$

where the transfer functions of $H_1(s)$–$H_4(s)$ are given in the Appendix. Substituting equation (19) into (20) gives

$$T_2(s) = \frac{H_1(s)H_3(s)}{1 - H_2(s)H_3(s)}T_0(s) + \frac{H_4(s)}{1 - H_2(s)H_3(s)}V_2(s). \tag{21}$$

It can be seen from equation (21) that the transfer function $G_1(s) = [H_1(s)H_3(s)]/[1 - H_2(s)H_3(s)]$ represents the input of pay-off model to the tension output of fiber, and the transfer function $G_2(s) = [H_4(s)]/[1 - H_2(s)H_3(s)]$ represents the velocity disturbance to the tension output of fiber. The coefficients of the polynomials in the transfer functions are dependent on the mechanical characteristics of the passive dancer roll, the fiber material properties, and the fiber velocity in the steady-state condition. Accurate system model is beneficial to controller design, but it is difficult to analyze the attenuation effect of dancer roll on disturbance intuitively using the $G_2(s)$, because it includes independent parameters m, b, k, B_f, and R. Thus, it is cumbersome and illogical to analyze the system using classical techniques. To reveal the inherent characteristics of passive dancer roll, it is necessary to explain the dancer roll simply and intuitively. Therefore, a simplified passive dancer model is established in this paper to illustrate the attenuation performance on the disturbance caused by velocity variation.

3. Analysis of Passive Dancer Roll

The linearized model of the passive dancer, presented in equation (21), is a fairly accurate model. In specific, the dynamics of the passive dancer is characterized by independent parameters, viz., $k, b, m, J_1, B_f, T_1, T_2$, and EA. Thus, to analyze the passive dancer roll using classical techniques, such as frequency response technique, each combination of the parameters should be considered to arrive at meaningful design guidelines for the dancer system. Such a linearized model can be used to design controllers, but is not clear for analysis, which is cumbersome and overwhelming. The dancer roll acts like a vibration absorber, and the disturbance is suppressed by the damped motion of the spring vibrator. Therefore, a free-body diagram of the passive dancer roll is developed in this section to illustrate the tension disturbance attenuation features of the dancer roll. The simplified model reflects the dynamic characteristics of the damped motion and ignores the fiber motion and roll rotation, which does not mean that these do not affect the tension control accuracy. It is usually necessary to equip guide rolls in consideration of the long travel of the fiber and the complicated mechanical mechanism. However, according to equation (17), the rotation of the guide roll is a delay link for the transfer of tension from upstream to downstream, which is not conducive to tension control. Therefore, the friction coefficient B_f of the dancer roll and its inertia J_1 will be as small as possible (the mass of the roll is not the same as "m," because "m" contains the mass of the slider used to install the roll, which do the damped motion together).

The simplified subsystem of the passive dancer roll is shown as Figure 4, assuming that the fiber is elastic. The upstream and downstream of the dancer roll are represented as springs, and the stiffness is K_1 and K_1, where $K_1 = EA/L_1$, $K_2 = EA/L_2$. So the tension in the fiber is equivalent to the spring force.

When the system is disturbed by the distance d from downstream, the force balance equation without passive dancer roll gives

$$K_1(X_1 + d_1) = K_2(X_2 + d_2), \tag{22}$$

where $d \triangleq d_1 + d_2$. The transfer function of upstream tension affected by disturbances without dancer roll can be expressed as

$$F_1(s) = K_1X_1(s) + \frac{K_1K_2}{K_1 + K_2}D(s), \tag{23}$$

where $F_1(s)$, $X_1(s)$, $D(s)$ are, respectively, the Laplace transforms of $F_1(t)$, $X_1(t)$, $d(t)$. The displacement of the dancer roll is assumed to be δx in the case of disturbance in the steady-state condition, so the dynamics of the translational motion of the dancer roll can be expressed as

$$(d_1 - \delta x)K_1 + (d_2 - \delta x)K_2 = m\ddot{\delta x} + b\dot{\delta x} + k\delta x. \tag{24}$$

The Laplace transform of equation (24) gives

$$\delta X(s) = \frac{2K_1K_2}{(K_1 + K_2)(ms^2 + bs + k + K_1 + K_2)}D(s). \tag{25}$$

So the transfer function of the upstream tension with passive dancer roll is expressed as

$$F_1'(s) = K_1X_1(s) + \frac{K_1K_2}{K_1 + K_2}D(s) \cdot \frac{ms^2 + bs + k + K_2 - K_1}{ms^2 + bs + k + K_1 + K_2}. \tag{26}$$

Similarly, the transfer function of downstream tension can be obtained as

$$F_2'(s) = K_2X_2(s) + \frac{K_1K_2}{K_1 + K_2}D(s) \cdot \frac{ms^2 + bs + k + K_1 - K_2}{ms^2 + bs + k + K_1 + K_2}. \tag{27}$$

In contrast (23) and (27), the dancer roll can attenuate the disturbance through its own motion, which acts as a filter. With equations (26) and (27), the following design guidelines can be got.

(i) If $k + K_2 < K_1$ or $k + K_1 < K_2$, the constant term of the transfer function is negative, which means the system is a nonminimum phase system and the nonminimum phase system has a larger phase lag, greatly limiting the stability and response ability of the system. So k should satisfy the condition $k > |K_1 - K_2|$. According to the assumption of the physical model, the fiber is linear elastic, and the equivalent spring can be modeled with stiffness constants, $K_1 = EA/L_1$ and $K_2 = EA/L_2$.

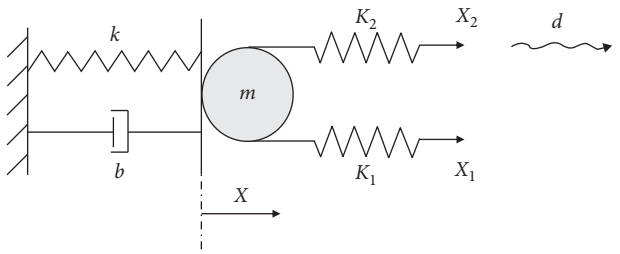

Figure 4: Simplified subsystem of the passive dancer roll.

(ii) According to equation (26), the dancer roll acts as a high-pass filter, attenuating the low-frequency disturbance, and the attenuation ratio can be expressed as $\eta = (k + K_2 - K_1)/(k + K_1 + K_2)$. When $k \longrightarrow \infty$, the dancer roll acts as a fixed guide roll, and no disturbance can be attenuated with $\eta \approx 1$. When $(k + K_2 - K_1) \longrightarrow 0$, $b \longrightarrow 0$, the dancer roll is the equivalent of an undamped inertial system, and the low-frequency disturbance can be completely attenuated with $\eta \approx 0$. However, a small disturbance will also lead to the continuous oscillation of the dancer roll for the undamped system.

(iii) The larger the value of $K_1 + K_2$, the smaller the attenuation ratio, and the better the attenuation effect achieved. So the passive dancer roll has better disturbance attenuation ability for the high modulus fiber materials. It is important to note that the higher modulus of the fiber will also be subjected to greater tension disturbance for the same $D(s)$, because the coefficient $K_1K_2/(K_1 + K_2)$ gets larger as well.

(iv) The smaller the η, the stronger the disturbance attenuation of the dancer roll, so the value of k should be as small as possible. The natural frequency of the spring oscillator system is $\sqrt{|k - K_1 - K_2|/m}$, and this frequency should be higher than that of any potential disturbance to avoid resonance. Therefore, it is necessary to select an appropriate large value of k and an appropriate small value of m when designing the passive dancer roll. The guideline makes a trade-off between the disturbance attenuation and resonance avoidance.

(v) The contrast equations (24) and (25) show that the degree of disturbance attenuation of the dancer roll to the upstream and that of the downstream are not the same. If $K_1 < K_2$, any motion of the dancer roll has a greater effect on the downstream, which is good for controlling the downstream tension. Consequently, $L_1 > L_2$ should be guaranteed when designing the dancer roll.

The design guidelines have been achieved. Considering the high-pass filtering characteristics of passive dancer roll, active dancer roll has been used to deal with high-frequency disturbances in some literatures [15, 16, 18], but it is not used in 16-Lane Fiber Placement End-effector because of its limitation.

Firstly, the frequency range of the disturbance attenuated by the active dancer roll depends on the bandwidth of the actuator of dancer roll, and the low-bandwidth actuator cannot respond to the disturbance at a frequency higher than its bandwidth. In practice, the bandwidth of actuators should be much higher than the frequency of potential disturbance to achieve good results. Secondly, regardless of the cost, actuators and measurement modules required by the active dancer roll should be integrated into the end-effector of AFP. These 16 sets of mechanisms will greatly increase the complexity and volume of the end-effector, thus not satisfying the placement of large curvature panels. In addition, the active dancer roll system includes the gearing mechanism that converts the rotary motion of the actuator into the linear motion of the dancer roll, and these complex motion pairs usually introduce nonlinear features such as clearance, friction, and so on, which complicates the control algorithm.

Comparing the characteristics of the two kinds of dancer roll, the passive dancer roll is adopted to attenuate the disturbance, and the guideline of the design is achieved base on the analysis of filtering performance. The mechanical parameters of the passive dancer roll are shown in Table 1. And then, the precision and robustness of the system are guaranteed by the tension closed-loop control of the pay-off motor.

4. Tension Control Design

The tension controller of the pay-off motor is designed using the H_∞ control framework as shown in Figure 5 with output weighting for the system G. K is the controller to be designed, T_2 is the output, Δu is the control signal, T_2^{ref} is the reference input, and e is the tracking error.

Define transfer functions S, R, and T:

$$S = (1 + KG)^{-1}, \tag{28}$$

$$R = K(1 + KG)^{-1}, \tag{29}$$

$$T = KG(1 + KG)^{-1} = 1 - S \tag{30}$$

where S is the sensitivity function, and T is the complementary sensitivity function. The sensitivity function S should be as small as possible for small tracking error; however, the complementary sensitivity function should be as small as possible for system robustness. The sum of these two should be 1, according to equation (28), so the values of S and T are functional in conflict. This problem can be described as

$$\left\| \begin{matrix} W_1S \\ W_2R \\ W_3T \end{matrix} \right\|_\infty \leq \gamma, \tag{31}$$

where W_1, W_2, and W_3 are all frequency-weighting functions. W_1 with "low-pass" characteristics has a high gain at low frequency to filter low-frequency disturbance. W_2, usually a weighting constant, can limit the control range. W_3

Table 1: Passive dancer roll parameters.

Parameter	Symbol	Value	Unit
Span 1	L_1	0.38	m
Span 2	L_2	0.33	m
Moving mass of dancer roll	m	0.5	kg
Damping of dancer roll	b	5	N/(m/s)
Spring stiffness	k	1000	N/m

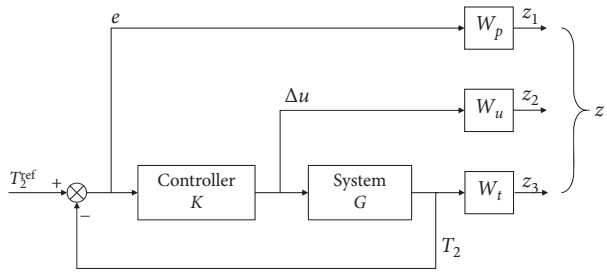

Figure 5: Block diagram of H_∞ framework.

with "high-pass" characteristics increases the attenuation of high frequency. The equations are as follows:

$$W_1(s) = \left(\frac{s/\sqrt[m]{M_S} + \omega_B}{s + \omega_B \sqrt[m]{A_s}}\right)^m,$$
$$W_3(s) = \left(\frac{s/\omega_{BT} + \sqrt[n]{M_T}}{\left(\sqrt[n]{A_T}/\omega_{BT}\right)s + 1}\right)^n, \quad (32)$$

where A_s is the steady-state error allowed, A_T is the maximum value of the system uncertainty, M_S and M_T represent the maximum peak magnitude of the S and T respectively, ω_B and ω_{BT} represent the required frequency bandwidth, m and n are adjusting parameters (usually, 1 is taken to obtain a small controller order).

The H_∞ tension controller is designed according to the dynamical performance requirements ($\omega_B = 139$ rad/s, $\omega_{BT} = 89.24$ rad/s, $M_S = 1.29$, $M_T = 1.13$, $W_2 = 0.2$). The values required for the calculation of the transfer function G_1 of system G are shown in Table 2. Using the MATLAB function HINFOPT, the controller $K(s)$ is computed using frequency-weighting functions above. Figure 6 illustrates the frequency response of the system.

5. Experiments for Tension Control System

Experiments of fiber control were carried out with the placement process of the AFP to verify the performance of the passive dancer roll and the H_∞ tension controller. The electrical structure diagram of fiber control system is as shown in Figure 7. The controller is realized based on BECKHOLL industrial personal computer and TwinCAT 3 software. The communication protocol is EtherCAT bus. The pay-off motor is AKM33e motor of Kollmorgen, and the tension sensor is DDE series of 50 N measurement range of AML.

The green arrows in Figure 8 represent the transmission line of the fiber feeding system, which is consistent with the structure in Figure 2. The end-effector of the AFP consists of 16 sets of fiber feeding mechanisms, each of which is equipped with a pay-off motor for controlling the fiber tension, a backing film motor for recovering the stripped backing film, a passive dancer roll, a tension sensor, and three guide rolls leading to the compaction roll. 16 sets of fiber are concentrated at the end of the compaction roll for placement.

Table 2: Fiber feeding system parameters.

Parameter	Symbol	Value	Unit
Young modulus of the fiber	E	0.16×10^9	N/m^2
Sectional area	A	6.35×10^{-7}	m^2
Nominal fiber tension	T_{10}, T_{20}	10	N
Nominal fiber velocity	V_{10}, V_{20}	1	m/s
Nominal radius of pay-off roll	R_0	0.1	m
Nominal weight of pay-off roll	m_0	5	kg
Radius of passive dancer roll	R_1	0.03	m
Radius of guide roll	R_k	0.02	m

The performance of passive dancer roll is compared at different fiber placement velocities and tensions. The value of acceleration represents the speed of velocity variation, which is the main source of disturbance in tension control. In addition, the nonroundness and eccentricity of rolls will also cause slight disturbance. The faster the fiber is, the higher the frequency of roll rotation will be, and the higher the disturbance frequency will be. Two sets of fiber are selected to carry on the contrast experiments: (1) the passive dancer roll is fixed as a guide roll; (2) the passive dancer is used for the disturbance attenuation equipment. The length of the panel mould used in the experiment is 4.8 m. The maximum velocity and acceleration of the AFP end-effector are 2000 mm/s and 2000 mm/s, and the information of the fiber placement velocity is obtained from the kinematic calculation of the axis of AFP. Reference tensions in experiments are 5 N, 10 N, and 15 N.

Figures 9–11 show the tension measured by tension sensor at different fiber velocities and reference tensions. Firstly, as can be seen from the figures, during the acceleration and deceleration stage of the fiber placement, the passive dancer roll effectively attenuate the disturbance from velocity variation by 30%–70%. As the acceleration value increases, the attenuation performance decreases slightly. Under the influence of the movement of dancer roll, although the peak value of tension fluctuation decreases greatly, the tension of fiber with passive dancer roll converges to the reference tension slower than that without dancer roll at steady fiber placement velocity.

The frequency of the disturbance caused by the nonroundness of the rolls increases with the increase of the fiber velocity at uniform fiber placement speed, and the attenuation effect of the passive dancer roll is reduced. In addition, the disturbance attenuation performance of the passive dancer roll is not affected by the change of the tension reference value, so it can adapt to the different tension requirements of the fiber placement process technology.

Overall, the experimental results show that the designed passive dancer roll can effectively attenuate the disturbance

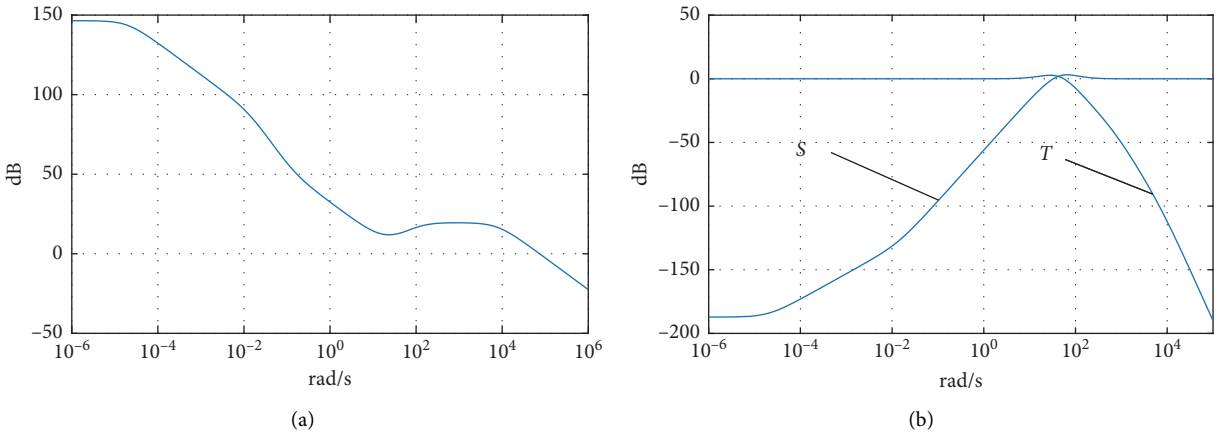

Figure 6: Bode diagram of H_{∞} tension controller: (a) controller, (b) functions S and T.

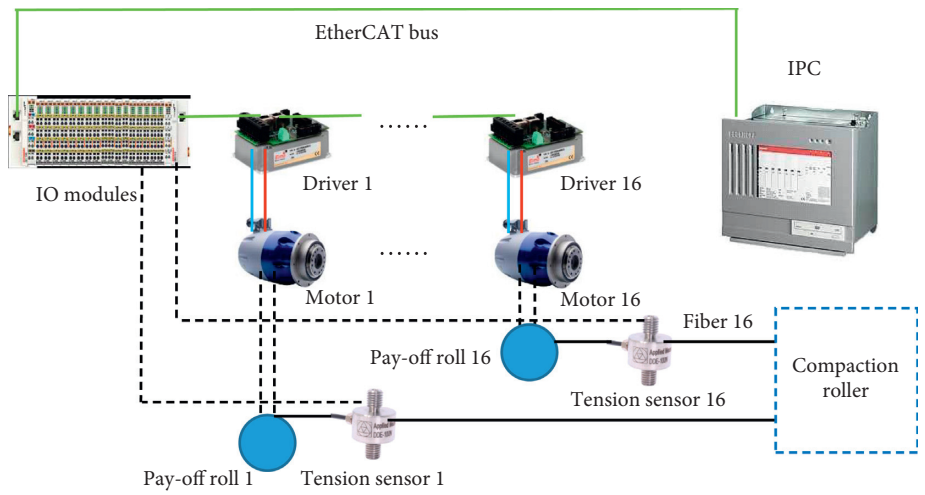

Figure 7: Electrical topologic structure.

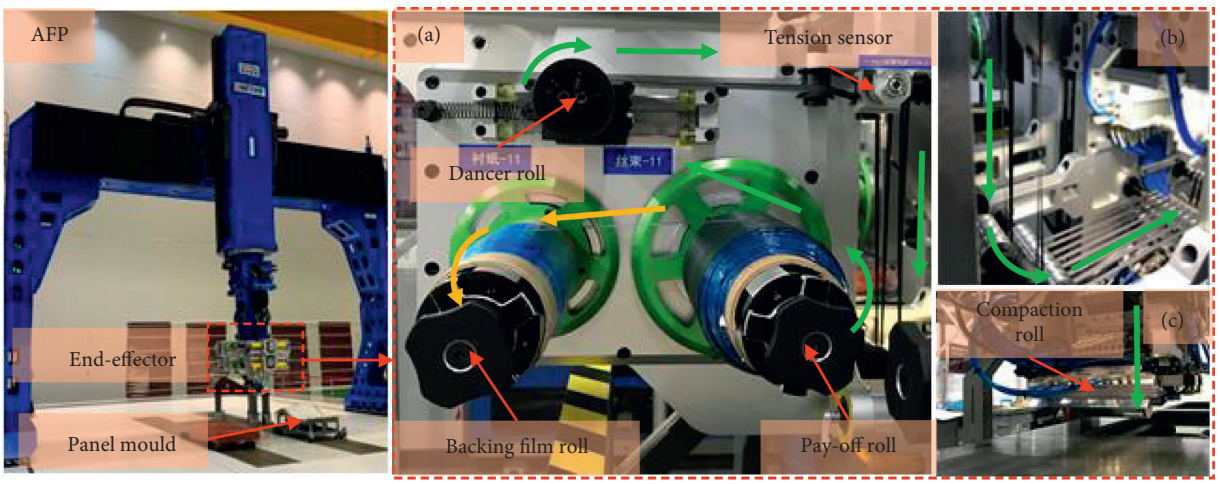

Figure 8: Fiber feeding system.

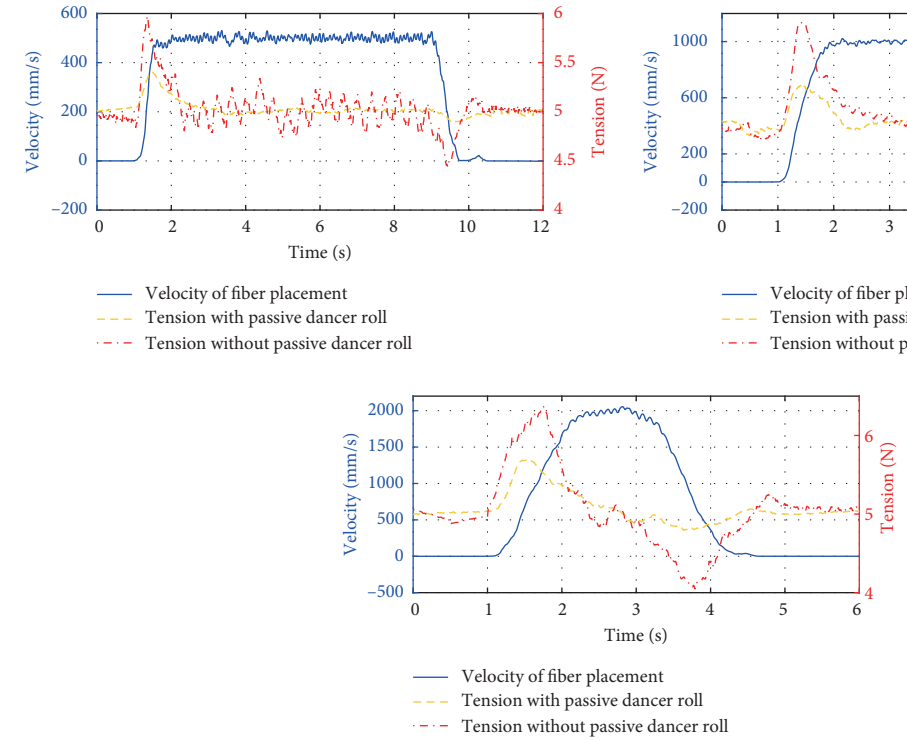

Figure 9: Experimental results at reference tension 5 N.

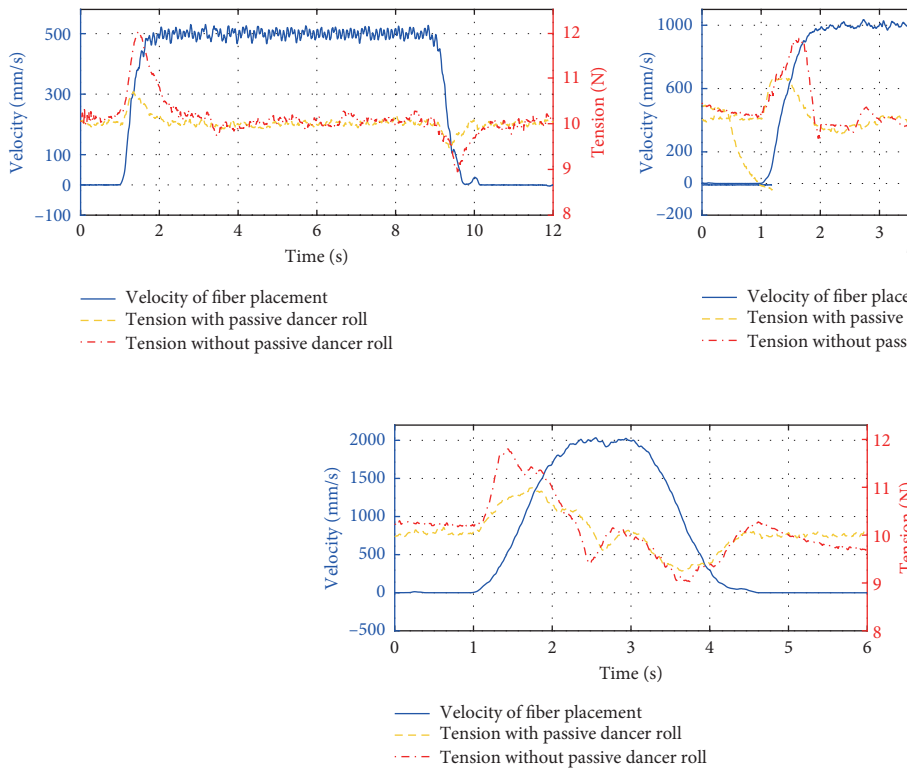

Figure 10: Experimental results at reference tension 10 N.

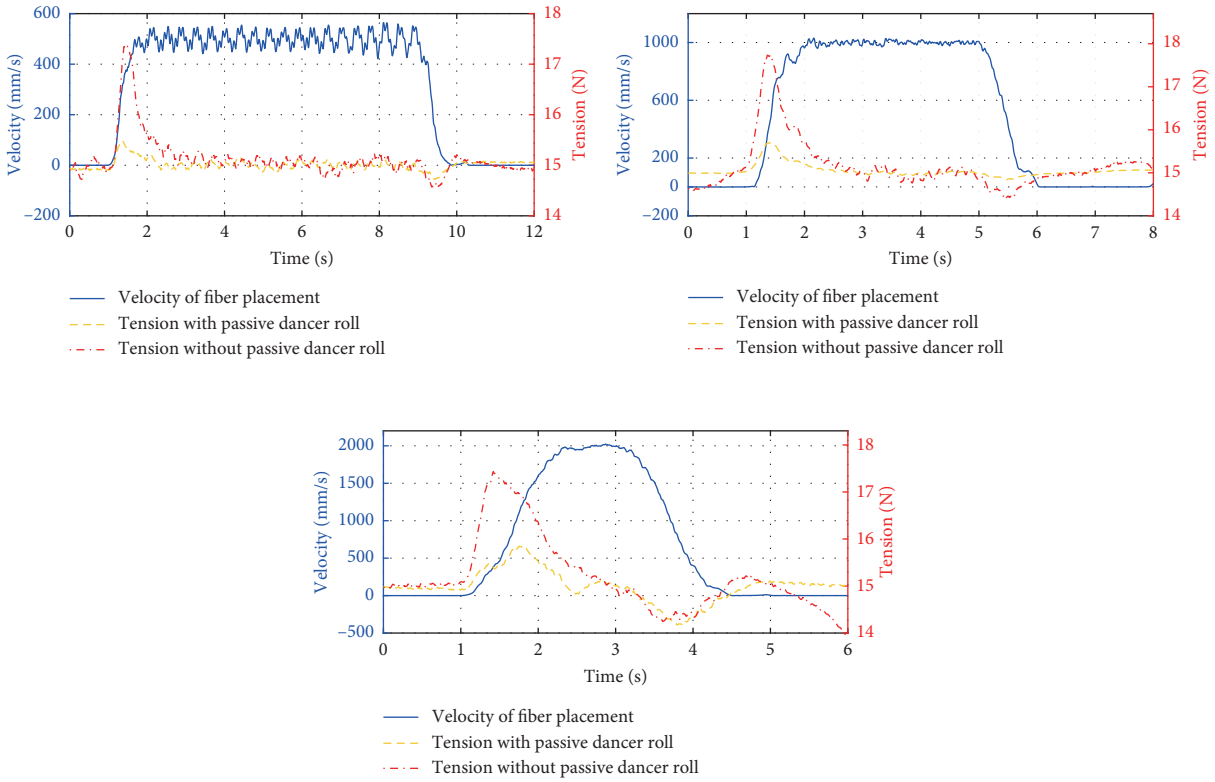

Figure 11: Experimental results at reference tension 15 N.

caused by the fiber placement velocity variation, especially in the low-frequency region, and it can make up the weakness of the insufficient bandwidth of the pay-off motor.

6. Conclusions

This paper designed an H_∞ tension control system with a passive dancer roll for the AFP machine and proposed design guidelines for the mechanical parameters of the passive dancer roll. Up to 16 sets of fibers are placed simultaneously, so it is impossible to accurately measure the placement velocity of each lane. The tension control system adopts a force closed-loop control strategy, employing the pay-off motor to control the fiber tension directly, and the tension feedback signal is measured by a tension sensor. The added passive dancer roll can regulate tension variations, which makes up the insufficient responsiveness of pay-off motor. It is necessary to research design guidelines of this dancer roll, and the simplified physical model shows the attenuation performance of the dancer roll to the velocity disturbance. Experimental results conducted on an AFP platform showed the robustness of the control system equipped with passive dancer rolls, with a steady-state error of 2%. The maximum fluctuation of tension did not exceed $1N$ under the disturbance of velocity change at the rate of $4\,\mathrm{m/s^2}$.

Appendix

Define $E_{10} = EA + T_{10}$, $E_{20} = EA + T_{20}$, $\alpha_0 = J_0 s + B_f/R_0$ and $\alpha_1 = J_1 s + B_f/R_1$

$$
\begin{aligned}
H_1(s) &= \frac{(ms^2 + bs + k)\left(E_{10}R_0^2 + \alpha_0 v_{00}\right)\alpha_1}{(ms^2 + bs + k)\left[\alpha_0\alpha_1\left(L_1 s + v_{00}\right) + \alpha_1 E_{10}R_0^2 + \alpha_0 E_{10}R_1^2\right] + \alpha_0\alpha_1 E_{10}s},\\
H_2(s) &= \frac{\alpha_0 E_{10}R_0^2(ms^2 + bs + k) - \alpha_0\alpha_1 E_{10}s/\sin\theta}{(ms^2 + bs + k)\left[\alpha_0\alpha_1\left(L_1 s + v_{00}\right) + \alpha_1 E_{10}R_0^2 + \alpha_0 E_{10}R_1^2\right] + \alpha_0\alpha_1 E_{10}s},\\
H_3(s) &= \frac{\left(E_{20}R_0^2 + \alpha_1 v_{10}\right)(ms^2 + bs + k) - \alpha_1 E_{20}\sin\theta s}{(ms^2 + bs + k)\left[\left(\left(L_2 s + v_{10}\right)\alpha_1 + E_{20}R_1^2\right)\right] + E_{20}\alpha_1 s},\\
H_4(s) &= \frac{E_{20}\alpha_1(ms^2 + bs + k)}{(ms^2 + bs + k)\left[\left(\left(L_2 s + v_{10}\right)\alpha_1 + E_{20}R_1^2\right)\right] + E_{20}\alpha_1 s}.
\end{aligned}
\tag{A.1}
$$

Data Availability

The data used to support the findings of this study are included within the article.

Conflicts of Interest

The authors declare that there are no conflicts of interest regarding the publication of this paper.

Acknowledgments

This work has been supported by the National Natural Science Foundation of China (Grant nos. 51975519 and 51775495).

References

[1] J. E. Green, "Overview of filament winding," *SAMPE Journal*, vol. 37, no. 1, pp. 7–11, 2001.

[2] H. J. L. Dirk, C. Ward, and K. D. Potter, "The engineering aspects of automated prepreg layup: history, present and future," *Composites Part B: Engineering*, vol. 43, no. 3, pp. 997–1009, 2012.

[3] B. Shirinzadeh, G. Alici, C. W. Foong, and G. Cassidy, "Fabrication process of open surfaces by robotic fibre placement," *Robotics and Computer-Integrated Manufacturing*, vol. 20, no. 1, pp. 17–28, 2004.

[4] C.-h. Tsai, C. Zhang, D. A. Jack, R. Liang, and B. Wang, "The effect of inclusion waviness and waviness distribution on elastic properties of fiber-reinforced composites," *Composites Part B: Engineering*, vol. 42, no. 1, pp. 62–70, 2011.

[5] N. Akkus and G. Garip, "Influence of pretension on mechanical properties of carbon fiber in the filament winding process," *The International Journal of Advanced Manufacturing Technology*, vol. 91, no. 9–12, pp. 3583–3589, 2017.

[6] X. Chen, Z. Zhu, G. Shen et al., "Tension coordination control of double-rope winding hoisting system using hybrid learning control scheme," *Proceedings of the Institution of Mechanical Engineers, Part I: Journal of Systems and Control Engineering*, vol. 233, no. 10, pp. 1265–1281, 2019.

[7] P. R. Pagilla, N. B. Siraskar, and R. V. Dwivedula, "Decentralized control of web processing lines," *IEEE Transactions on Control Systems Technology*, vol. 15, no. 1, pp. 106–117, 2007.

[8] T. T. Tran and K. H. Choi, "A backstepping-based control algorithm for multi-span roll-to-roll web system," *The International Journal of Advanced Manufacturing Technology*, vol. 70, no. 1–4, pp. 45–61, 2014.

[9] K.-H. Choi, T. T. Tran, and D.-S. Kim, "Back-stepping controller based web tension control for roll-to-roll web printed electronics system," *Journal of Advanced Mechanical Design, Systems, and Manufacturing*, vol. 5, no. 1, pp. 7–21, 2011.

[10] T. T. Tran, K.-H. Choi, D.-E. Chang, and D.-S. Kim, "Web tension and velocity control of two-span roll-to-roll system for printed electronics," *Journal of Advanced Mechanical Design, Systems, and Manufacturing*, vol. 5, no. 4, pp. 329–346, 2011.

[11] M.-T. Yan, "Modelling and adaptive control of the wire transport system in wire electrical discharge machining," *Proceedings of the Institution of Mechanical Engineers, Part I: Journal of Systems and Control Engineering*, vol. 218, no. 8, pp. 637–643, 2004.

[12] K. H. Shin, *Distributed control of tension in multi-span web transport systems*, Ph.D. thesis, Oklahoma State University, Stillwater, OK, USA, 1991.

[13] N. A. Ebler, R. Arnason, G. Michaelis, and N. D'Sa, "Tension control: dancer rolls or load cells," *IEEE Transactions on Industry Applications*, vol. 29, no. 4, pp. 727–739, 1993.

[14] J. J. Shelton, "Limitations to sensing of web tension by means of roller reaction forces," in *Proceedings of the Fifth International Conference on Web Handling*, Stillwater, OK, USA, 1999.

[15] H.-K. Kang, C.-W. Lee, K.-H. Shin, and S.-C. Kim, "Modeling and matching design of a tension controller using pendulum dancer in roll-to-roll systems," *IEEE Transactions on Industry Applications*, vol. 47, no. 4, pp. 1558–1566, 2011.

[16] R. V. Dwivedula, Y. Zhu, and P. R. Pagilla, "Characteristics of active and passive dancers: a comparative study," *Control Engineering Practice*, vol. 14, no. 4, pp. 409–423, 2006.

[17] V. Gassmann, D. Knittel, P. R. Pagilla et al., "Fixed-order H_∞ tension control in the unwinding section of a web handling system using a pendulum dancer," *IEEE Transactions On Control Systems Technology*, vol. 20, no. 1, pp. 173–180, 2012.

[18] C. Thiffault, P. Sicard, and A. Bouscayrol, "Desensitization to voltage sags of a rewinder by using an active dancer roll for tension control," in *Proceedings of the IEEE International Conference on Electric Machines and Drives*, IEEE, San Antonio, TX, USA, pp. 466–473, May 2005.

[19] H. Koc, D. Knittel, M. de Mathelin, and G. Abba, "Modeling and robust control of winding systems for elastic webs," *IEEE Transactions on Control Systems Technology*, vol. 10, no. 2, pp. 197–208, 2002.

[20] K. H. Shin, J. I. Jang, H. K. Kang et al., "Compensation method for tension disturbance due to an unknown roll shape in a web transport system," *IEEE Transactions on Industry Applications*, vol. 39, no. 5, pp. 1422–1428, 2003.

[21] K. Choi, M. Zubair, and G. Ponniah, "Web tension control of multispan roll-to-roll system by artificial neural networks for printed electronics," *Proceedings of the Institution of Mechanical Engineers, Part C: Journal of Mechanical Engineering Science*, vol. 227, no. 10, pp. 2361–2376, 2013.

[22] G. Xie, J. Wang, W. Chen et al., "Tension control in unwinding system based on nonlinear dynamic matrix control algorithm," in *Proceedings of the 12th IEEE Conference on Industrial Electronics and Applications*, IEEE, Siem Reap, Cambodia, pp. 1230–1235, June 2017.

[23] H. Zhang, H. Tang, and Y. Shi, "Precision tension control technology of composite fiber tape winding molding," *Journal of Thermoplastic Composite Materials*, vol. 31, no. 7, pp. 925–945, 2018.

[24] P. Zhao, Y. Shi, and J. Huang, "Dynamics modeling and deviation control of the composites winding system," *Mechatronics*, vol. 48, pp. 12–29, 2017.